A FRAMEWORK FOR FEEDBACK CONTROL OF STRESS USING EEG AND AUDIO

A Thesis

Presented in Partial Fulfillment of the Requirements for the Degree Bachelor's of Science with Honors Research Distinction in the College of Engineering of The Ohio State University

By

Kevin P. Everson,

* * * * *

The Ohio State University

2018

Thesis Committee:

Kevin M. Passino, Adviser

Lee C. Potter

Approved by

Adviser

Bachelor's of Science in Electrical & Computer Engineering

ABSTRACT

Mood disorders, which are greatly affected by stress, are at the forefront of health concerns confronting the world today. This research introduces and evaluates a framework for feedback control of stress using audio stimuli and electroencephalography sensing. We propose a control system configuration which includes calibration of stress based on brain activity in each trial via a regression model. Next, the input-output mapping between music characteristics and stress is modeled as a dynamical system, and validation results are provided that indicate that this relationship can be approximated by a linear model. Finally, we assess the outcomes of preliminary proportional control testing. Hopefully, the findings of this research can stimulate future investigation of the use of feedback control for emotion regulation that will have a positive effect on mood disorders.

This is dedicated to my parents, for every ounce of unconditional love and devotion they have given to their children.

ACKNOWLEDGMENTS

First and foremost, I must thank my family, immediate and extended, whose support has paved the academic path on which I find myself.

I owe my sincerest gratitude to my adviser, Professor Kevin M. Passino, for sharing his immense wisdom during nearly my entire undergraduate career. His technical expertise and commitment to the use of engineering as a tool for the benefit of humanity have served as constant sources of inspiration to me.

Hugo González Villasanti, for his invaluable qualities as a teacher, a mentor, and a friend. Working with him over the past three years has truly been one of the most incredible privileges I could have hoped for, and I am eager to witness the positive impact that he creates during his career. To this project, he was a resource in many areas, especially in conceptualizing the systems at play and how they should be analyzed.

Because my research is highly connected with the work of many others in this group, I would be remiss not to mention the contributions of these individuals. In particular, I acknowledge Professor Andrés Darío Pantoja Bucheli for his input on music modulation and system identification that has often guided me in recent months.

Finally, I thank Professor Lee C. Potter for his willingness to be a member of my undergraduate thesis committee.

VITA

8 March 1996 ..... Born - Cincinnati, Ohio

16 December 2018 ..... B.S., Electrical & Computer Engineering, The Ohio State University

FIELDS OF STUDY

Major Field: Electrical & Computer Engineering

Undergraduate Program of Study: Electrical Engineering

TABLE OF CONTENTS

Page

LIST OF FIGURES

Figure **Page**

CHAPTER 1

INTRODUCTION & BACKGROUND

1.1 Emotion Elicitation & Regulation

Of all health crises plaguing the world today, mental health issues are among the most pressing. Mood disorders such as major depressive disorder, bipolar disorder, and generalized anxiety disorder are incredibly prominent across the globe, with over 25% of the world's adult population developing one or more mood or behavioral disorders over the course of a lifetime [14]. In many cases, these disorders can have a cyclical relationship with addiction [21] and self harm, and can possibly lead to suicide. Given the prevalence of these mood and emotional disorders and their possibly fatal consequences, the fields of emotion measurement, elicitation, and regulation merit thorough investigation.

Various methods have been used for the measurement and interpretation of emotion. Perhaps the most common approaches arise socially, in verbal (self-reporting) or non-verbal (facial expressions, laughter) cues. While these methods are satisfactory in many diagnostic settings, they can be impossible to quantify and it is thus difficult to properly evaluate the dynamics of mood and emotion based on these indicators alone. As a result, several studies have investigated techniques of psychophysiological

characterization of emotion. Some such methods include rate of respiration, hormone secretion, and skin temperature [8].

Via any valid approach to measuring emotion, it is possible to evaluate the effectiveness of a stimulus in eliciting emotion. For example, studies often expose subjects to a standardized series of images called the International Affective Picture System (IAPS), to measure emotion along three dimensions: valence, arousal, and dominance. By recording the emotional response of a large sample of subjects, through various methods of measurement, the relationship between input (image stimuli) and output (emotional response) can be rigorously investigated [1]. Similarly, characteristics of music have been linked to the elicitation of specific emotions. Studies such as [2] and [8] have thoroughly researched this relationship, and the emotional effects of elements such as volume, pitch, pitch contours, mode, tempo, and others have been illustrated.

Due to the aforementioned prevalence and importance of mood disorders, as well as the investigation of emotion elicitation and measurement, the field of emotion regulation, both intrinsic (internal regulation of one's own emotions) and extrinsic (regulation of one's emotions via external stimuli), has received significant attention. A model of emotion regulation from [3] is shown in Fig. 1.1.

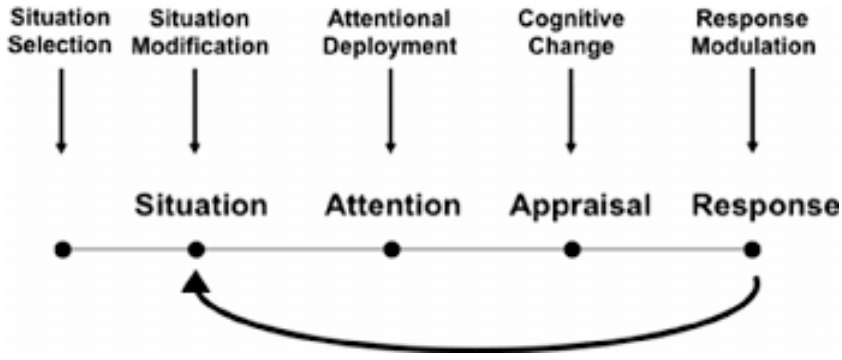

Figure 1.1: Emotion regulation process model [3].

Here, a subject chooses to engage in and/or alter an external or internal environment, directs his attention towards a certain stimulus and reacts cognitively, and subsequently responds (e.g., emotionally and behaviorally) to this change. This response can then alter the original situation. The significance of emotion regulation with respect to mood disorders has been comprehensively investigated. For example, whereas reappraisal of a situation typically results in lower depression severity, rumination and suppression lead to greater severity. To summarize, "regulation of negative moods and emotions play a significant role in the onset and maintenance of mood disorders" [7]. The continued study of effective emotion regulation strategies is therefore essential to reducing prevalence of mood disorders.

1.2 Electroencephalography

To measure an emotional state, an appropriate sensor must be chosen. Many strategies have been studied for measuring stress. For example, studies such as [9] have shown that stressful stimuli can induce a change in conductance of a subject's

skin, commonly known as a galvanic skin response (GSR). Other studies [17] have linked lower heart-rate variability (HRV) to higher stress.

The sensor used in this research was the electroencephalograph (EEG). As neurons fire differently in various areas of the brain, electrical potentials changes. The EEG instrument measures this electrical activity using electrodes placed on the scalp. By recording the changing potential difference between electrodes, the EEG can create a time-domain plot of the electrical potentials for each electrode, known as an electroencephalogram (also known as "EEG", but the term "EEG recording" will be used henceforth for clarity) [19]. For most of its history since its inception during the early 20th century, the EEG used the electrical activity directly from the brain to fluctuate a writing utensil on a moving paper chart. Fortunately, this information can now be recorded and processed digitally.

Characterization of brain activity recorded by an EEG requires focusing on important information. Relevant items characterizing brain activity are the amplitude, frequency and location of changing electric potential.

The varying electrical potential signals in an EEG recording are often divided into frequency bands. While the exact bounds of these bands may vary based on source or application, they are generally accepted to be the approximate ranges shown in Table 1.1. The energy in these bands is a fundamental piece of information used in extraction of information from an EEG signal.

Meanwhile, observing the location of EEG data gives insight into activity in different areas of the brain.

Band	Frequency (Hz)
Delta	< 4
Theta	$4 - 8$
Alpha	$8 - 13$
Beta	$13 - 30$
Gamma	$30 - 100$

Table 1.1: EEG data frequency bands.

Previous Research

While electroencephalography is often used in studying conditions such as epilepsy and sleep disorders, many have studied its utility in measuring emotion. Some such studies propose a Higuchi Fractal Dimensional model using EEG data for emotion estimation, to varying degrees of success. For example, [6] exposed subjects to audio-visual stimuli, and compared their EEG brain activity to the intrinsic emotional characterization of the stimuli (similar to the IAPS experiment), as well as the subject's self-reported emotional state. The best models in this study achieved 88% and 83% accuracy in classifying a subject's arousal and valence, respectively, based on their recorded brain activity. One experiment, though unrelated to the study of emotion, did use brain activity for feedback control. In [16], subjects were maintained at a stable level of sedation using EEG data to monitor their anesthesia needs.

From the conceptualization shown in Fig. 1.1, it is evident that the dynamics of emotion regulation share many properties with the systems examined in the field of controls–there is an input/output relationship, which is influenced by a feedback mechanism. In addition, studies have clearly shown the utility of EEG data in estimating emotional states. Thus, the goal of this research was to examine the input/output

relationship between a stimulus and emotional state using EEG sensing. In this case, music was chosen as the input and stress was chosen as the output, due to the wealth of literature and intuitive understanding surrounding the nature of ability of music to elicit/reduce stress. While other emotional descriptions may have more complex relationships to musical characteristics, the response of stress is generally more clear.

In Chapter 2, we discuss the equipment used in this thesis. Primarily, this includes the Emotiv EPOC+ EEG headset. In addition, the functionality of the EmotivPRO software, data acquisition code, and of the Stroop interference test are described.

In Chapter 3, the control framework and system evaluation are examined. First, a regression model for the relationship between EEG band-power data is described. Then, system models mapping two audio characteristic inputs (average pitch and average volume) to a stress output are evaluated. Finally, we outline methods for real-time modulation of audio signals.

In Chapter 4, the broader conclusions and implications of this research are discussed.

CHAPTER 2

LABORATORY EQUIPMENT

2.1 Emotiv EPOC+ EEG Headset

EEG instruments vary in terms of utility and cost. Less expensive products typically consist of fewer than ten normally dry electrodes. Often tailored for consumer use, they are priced for just a few hundred dollars. Higher-end devices, on the other hand, can run upwards of $25,000 and have anywhere from 32 to a few hundred electrodes which may require conductive gel or paste. The improved data provided by these devices is often necessary for medical settings. The Technology 4 Mental Health group has access to a number of EEG headsets, including the Wearable Sensing DSI 7, OpenBCI EEG Headband, Emotiv Insight, and Emotiv EPOC+ devices.

The device used for the majority of this research was the Emotiv EPOC+, seen in Fig. 2.1. Situated between consumer and medical-grade instruments in terms of price and quality, the EPOC+ is suitable for many research applications. This device features fourteen electrodes consisting of metal contacts and felt sensors which must be soaked in a saline solution for adequate contact quality. Given its relatively small size, rechargeable battery, and ability to transmit collected data via Bluetooth, it is fairly mobile and can be worn by a subject without excessive discomfort. Thus, it

strikes an optimal balance between form and function. Its bandwidth is $0.2 - 45$ Hz, which captures all relevant frequencies between the Delta and Gamma bands [4].

The EPOC+ also includes an accelerometer and gyroscope, which captures motion data that is used in interactive purposes.

Figure 2.1: Emotiv EPOC+ [4].

The Emotiv Insight EEG, seen in Fig. 2.2, was also used during some preliminary experiments. While it is an even lighter headset and does not use wet sensors, its acquired data was found to be less useful and reliable than the data collected by the EPOC+.

Figure 2.2: Emotiv Insight [5].

2.2 EmotivPRO

Emotiv Inc. also provides software for use in conjunction with their physical EEG instruments. This suite of software includes EmotivPRO for Windows and Mac operating systems, "My Emotiv" for iOS and Android, various interactive apps, as well as a software development kit (SDK).

The Emotiv EEG headset can send raw EEG data that it produces to a computer via Bluetooth at a user-configurable rate of 128 or 256 Hz, where they can then be observed and recorded in EmotivPRO. The raw EEG data interface of EmotivPRO

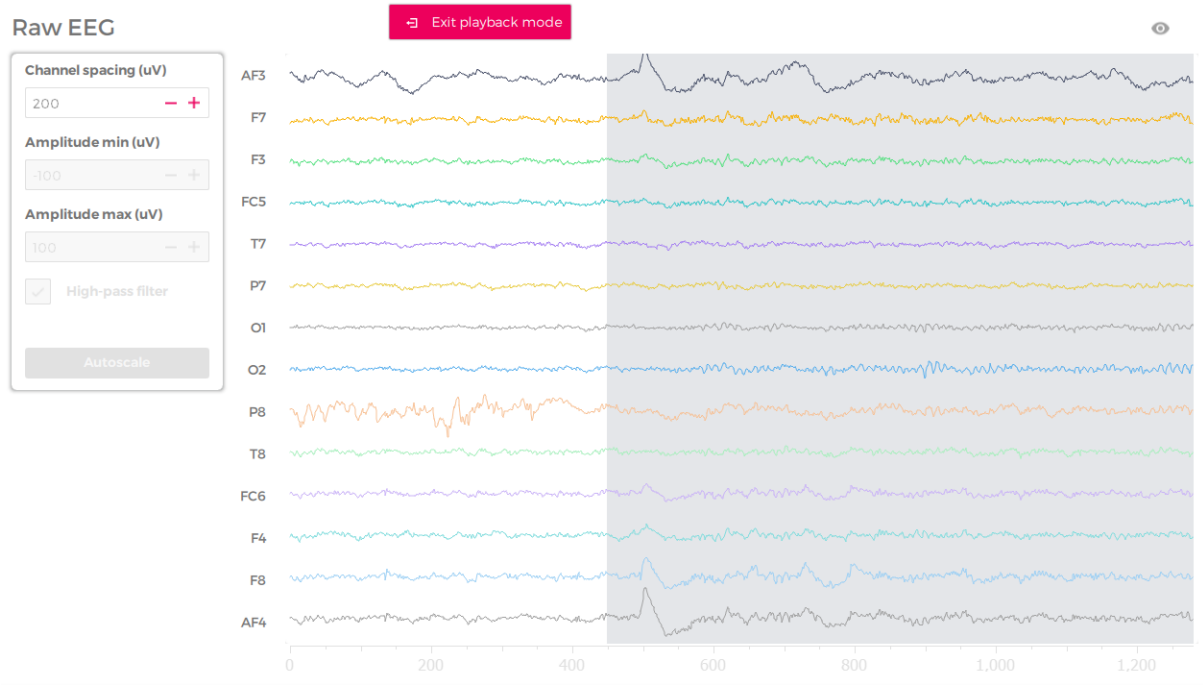

Figure 2.3: EmotivPRO raw EEG interface.

is displayed in Fig. 2.3, and shows a plot of the electric potential at each electrode vs. time. This raw data can be exported to an .edf or .csv file.

By using window functions on segments of raw data from each electrode, EmotivPRO computes the power in various frequency bands at a sampling frequency of 8 Hz. For each of the fourteen electrodes, the band-power data interface of EmotivPRO shown in Fig. 2.4 displays a real-time fast Fourier transform plot of the windowed raw data, as well as the power in each of five frequency bands: Theta ($4-8$ Hz), Alpha ($8-12$ Hz), Low Beta ($12-16$ Hz), High Beta ($16-25$ Hz), and Gamma ($25-45$ Hz). These are approximately in line with the bounds displayed in Table 1.1.

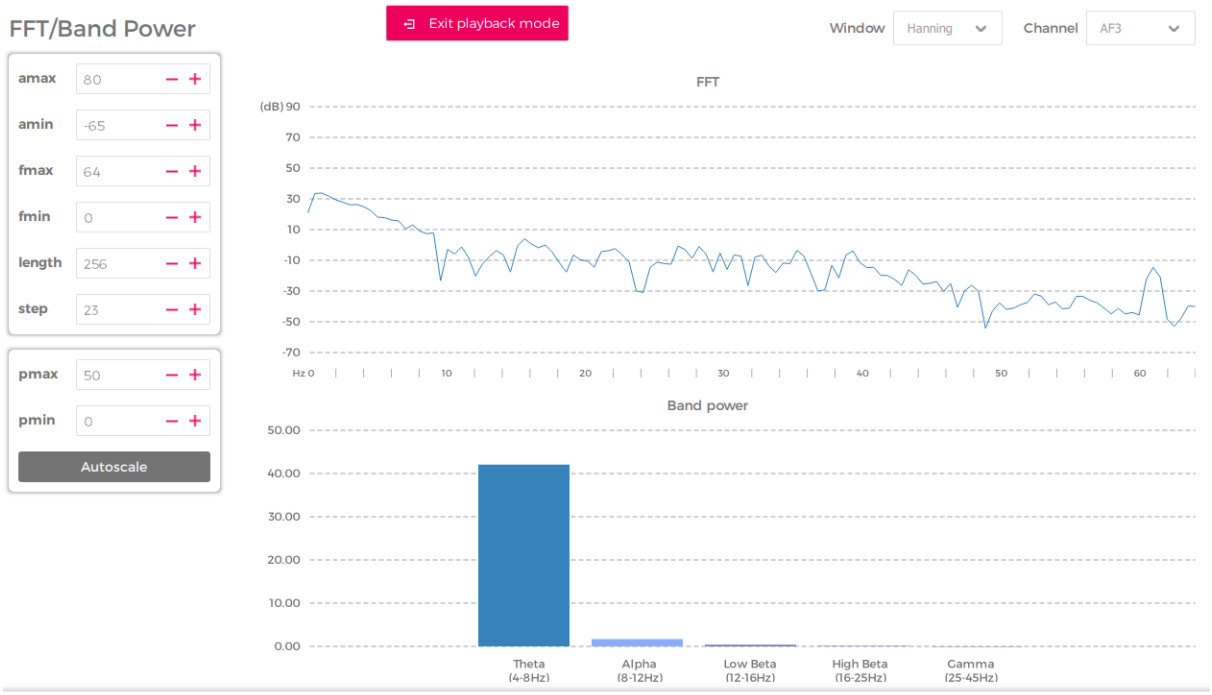

Figure 2.4: EmotivPRO band-power data interface.

These data can be viewed separately for each of the fourteen electrodes, using five window types: Hanning (sic), Hamming, Hann, Blackman, and rectangle, depending on the user's resolution and sidelobe suppression needs.

When starting this project, Emotiv did not allow this data to be exported, so time was dedicated to creating bandpass filters that divided the raw data into desired frequency bands. Fortunately, the company later released an update that permitted the export of band-power data, using the Hanning window.

Performance metrics are the last relevant data type provided by EmotivPRO. These process the collected EEG data to quantify six emotional states exhibited by the user (stress, engagement, interest, excitement, focus, and relaxation) on a scale

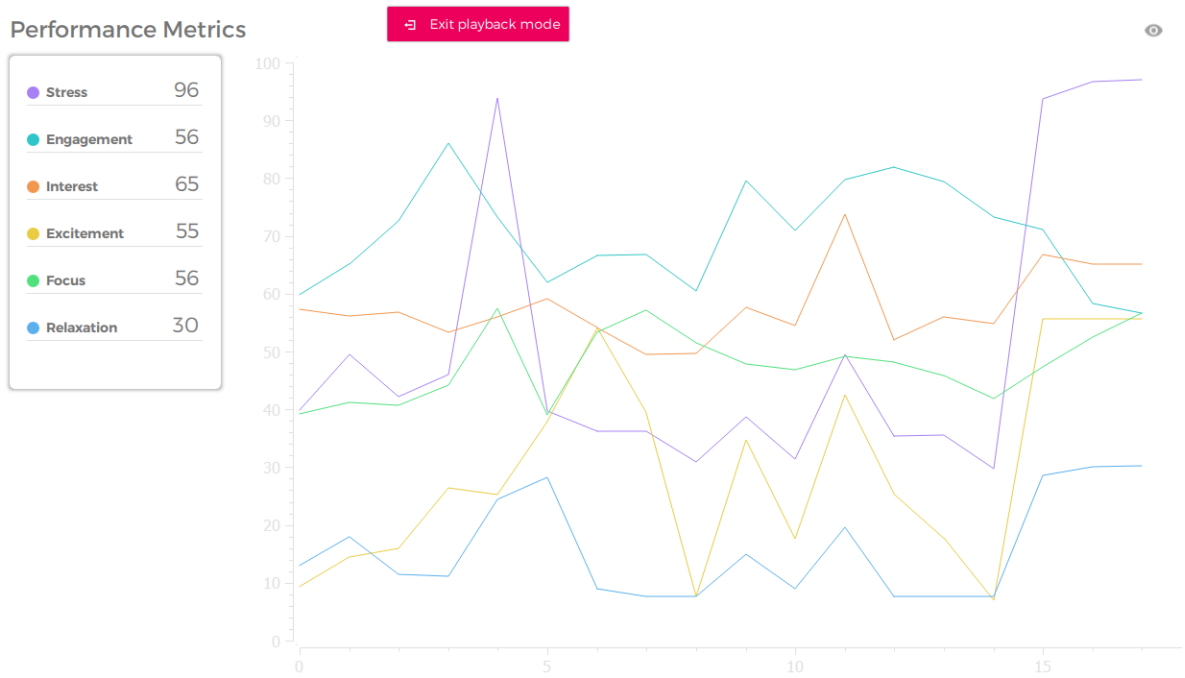

Figure 2.5: EmotivPRO performance metric data interface.

of $1 - 99$ at a rate of 0.1 Hz. The performance metric data interface can be seen in Fig. 2.5.

Being proprietary software, the exact method that EmotivPRO uses to compute these performance metrics has not been fully disclosed. It was hypothesized that Emotiv Inc. used data, either self-reported or collected via other means (heart rate, HRV, etc.) to create a model of determining these emotional states based on EEG data that is reasonably representative of the average subject.

Like the band-power data, the performance metric data originally could not be exported, but the ability to export was added during the same software update. It is worth noting that the exported performance metric data contains two values for each emotion type: "raw" and "scaled". The raw value is automatically generated

from the other EEG data, with a lower bound of 0 and an unspecified upper bound. Meanwhile, the scaled value fits the raw data to a $0-1$ range based on the minimum and maximum raw values during a recording. The performance metric data interface in Fig. 2.5 uses these scaled values.

2.3 Data Acquisition

While EmotivPRO allows for easy observation, collection, and export of EEG data, the goal of this project is to provide a platform for feedback control using EEG data as an output. Therefore, simply recording data in EmotivPRO and exporting it was not adequate because a control input cannot be modulated in real-time.

Raw EEG, band-power, and performance metric data can be gathered using the Emotiv SDK in C++, C#, Objective-C, Python, Java, and MATLAB. A program was written in MATLAB to acquire the stress performance metric (both scaled and raw), which can be used in real-time. The band-power data can also be captured in real-time using the SDK.

2.4 Stroop Interference Test

Because every subject may have a different reaction to stress, a standard stimulus was necessary in order to observe each subject's stress response. The Stroop interference test was chosen for this standardization. In this task, the subject is presented with text of a color, which itself is printed in a color that may or may not be the same as the one that is written. The subject must enter a key corresponding to the color of the printed text, rather than the word itself. This procedure is demonstrated

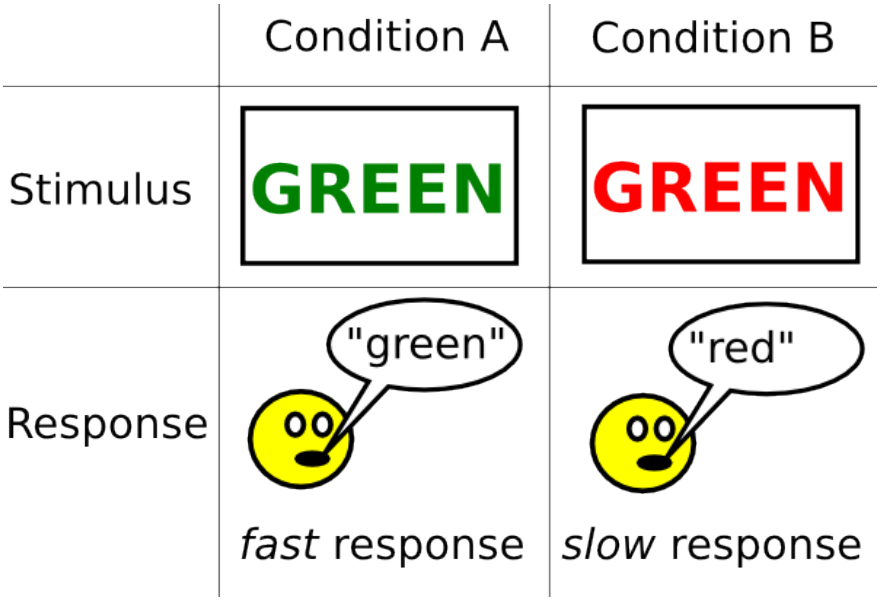

Figure 2.6: Stroop interference test example [15].

in Fig. 2.6. Using the tools provided by [15], a Stroop task experiment was coded, lasting approximately two minutes.

The conflicting information presented to the subject during a Stroop test has been proven to induce confusion and stress, and the ubiquity of the Stroop effect in research made it especially attractive and convenient for our purposes. For instance, the experiment performed in [18] tracked the subjects' psychological, physiological, muscular, and hormonal responses to the Stroop test, and recorded significant changes as a result of the stimulus, indicating that the Stroop test is suitable for studying stress-responses.

CHAPTER 3

CONTROL FRAMEWORK

Before constructing a feedback controller around a dynamical system, the system must be conceptualized and understood. In this case, the system was conceptualized as in Fig. 3.1. Here, a desired reference stress level is defined as $r(k)$. Comparing this reference level to the actual current stress level, an audio signal $u(k)$ is modulated and streamed. The brain's electrical activity in response to the stimulus is recorded by an EEG instrument. This raw data can be transformed to the frequency domain for more useful information extraction. Finally, this band-power data can be used to approximate stress, which is then fed back to the controller.

While our analysis of this system may consider a single input $u(k)$ to the plant, in reality the brain has many other concurrent inputs that may induce changes in stress. Thus, $w(k)$ represents these other influences, or disturbances. It is also important to remember that while this system was analyzed as a linear time-invariant (LTI) system, the brain is not LTI.

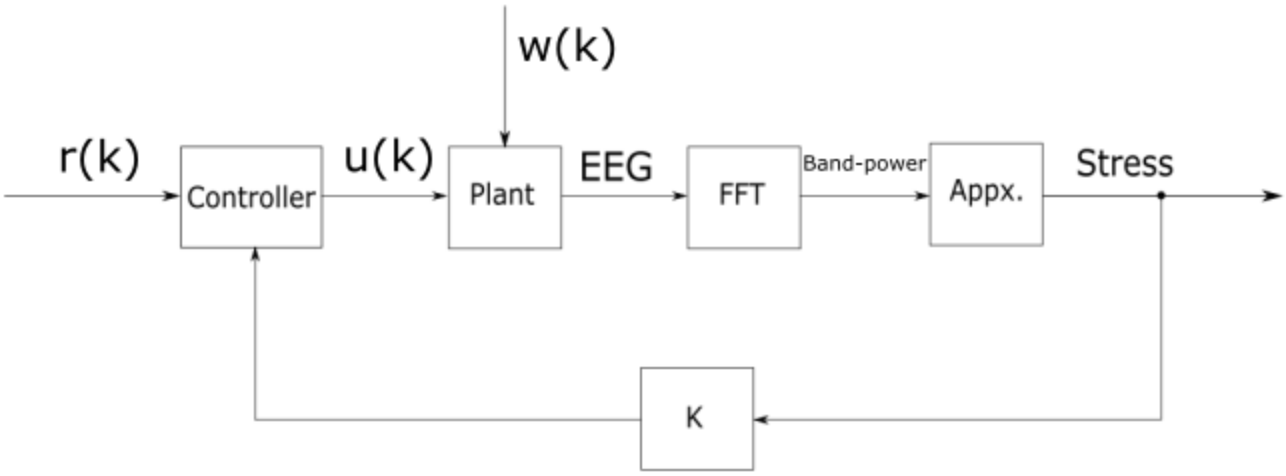

Figure 3.1: Control system configuration.

3.1 System Dynamics & Testing

Experimental Design

An experiment was devised to evaluate the relationship between music and stress. However, because each subject may react differently to stress-inducing stimuli, and even the same subject may react differently in two different trials, the relationship between EEG band-power data and stress must be first calibrated. Thus, the experiment comprised of two stages. In stage one, the subject underwent alternating two-minute intervals of rest and Stroop test stimuli. In stage two, the subject listened to an audio track–in this case, "Notturno", recorded by the Royal Philharmonic Orchestra [13]. The experiment layout can be seen in Fig. 3.2.

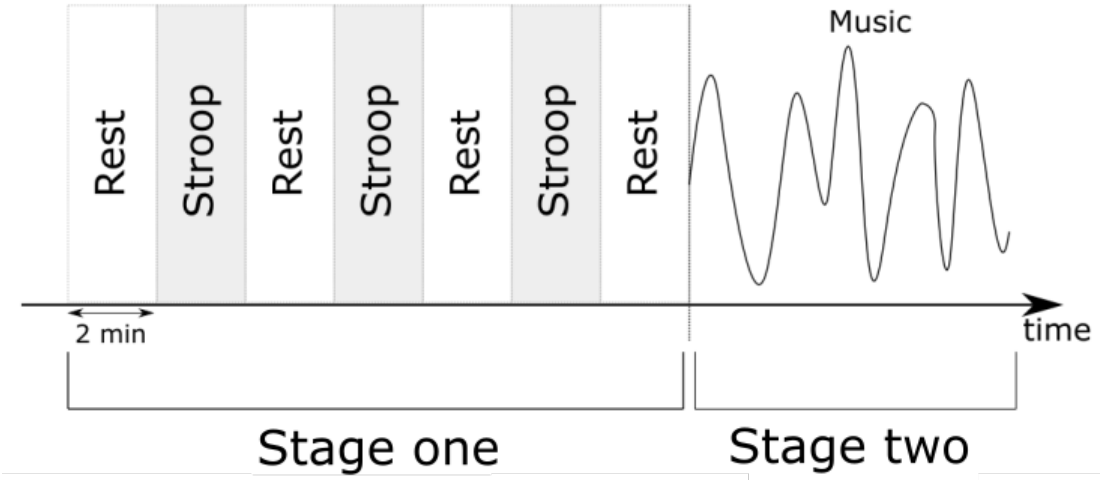

Figure 3.2: Experiment layout.

From both stages of the experiment, the subject's EEG band-power data was recorded (fourteen electrodes, five frequency bands per electrode for a total of 70 values per time sample). In stage two, the Matlab MIRtoolbox was used to compute the average pitch and volume for the entire audio track over segments of a specified length. In this case, the audio frame length was chosen as one second in order to avoid excessive noise while still adequately capturing the audio characteristics. Thus, from stage two, the average pitch and volume over one-second frames were recorded for the entire track using *mirpitch*() and *mirrms*() respectively [10].

For current and future reference, the average pitch, volume, and approximated stress for stage two of the experiment are plotted in Fig. 3.3.

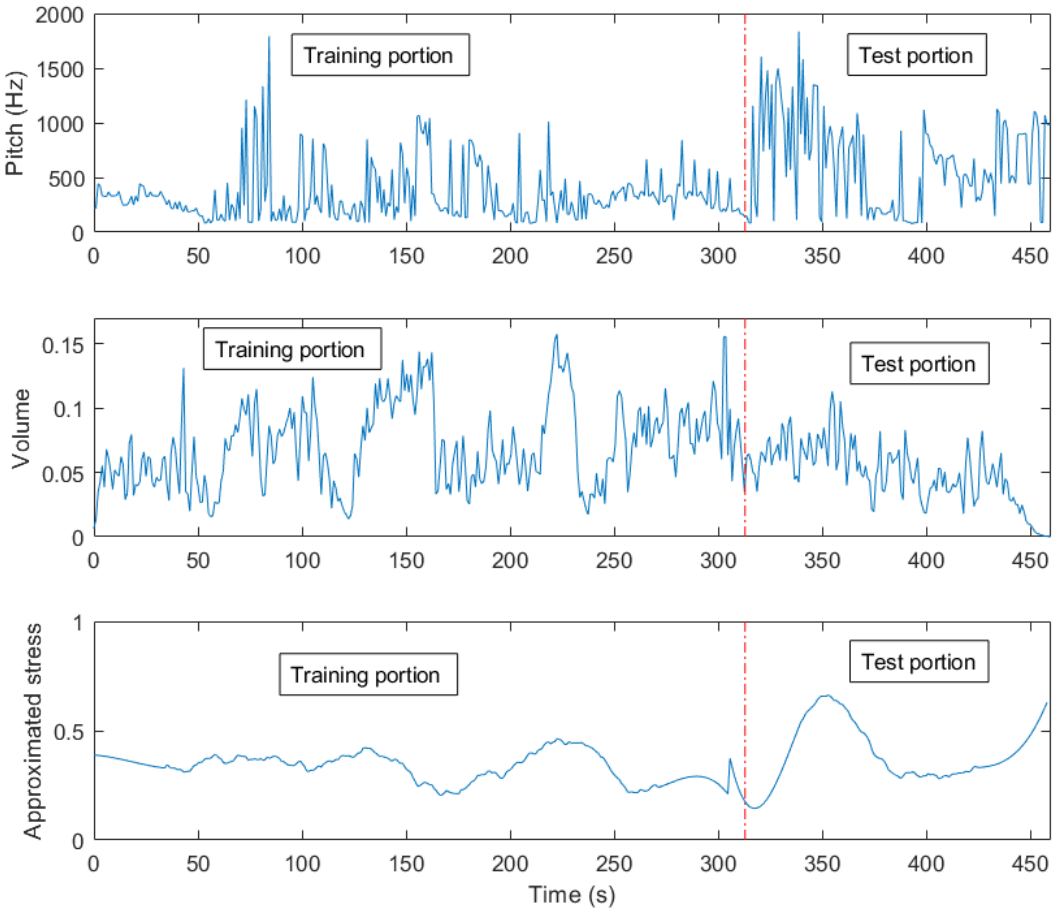

Figure 3.3: Average pitch, average volume and approximated stress vs. time for stage two of the experiment.

From this plot, the trends in approximated stress can possibly be attributed to the audio characteristics at a few points in time. For example, local maxima in approximated stress near the ~ 130, ~ 220, ~ 305, and ~ 350 second times appear to coincide with increases in pitch and/or volume. This relationship will be explored further in the following subsections.

Band-power to Stress Calibration

Before analyzing the influence of the music input $u(k)$ on stress, it is important to determine the relationship between band-power data and stress for each trial. The subsystem in question is shown in Fig. 3.4, and uses data collected from stage one of the experiment.

Figure 3.4: Band-power to stress conceptualization.

First, the band-power data recorded during stage one was decimated to a sampling frequency of 1 Hz, such that it lined up with the time indices of pitch and volume obtained in stage two. Next, a "ground truth" stress value of zero was assigned for each period of rest, while a stress value of one was assigned for the periods of time in which the subject underwent the Stroop test stimulus. This ground truth stress signal was thus a square wave, also with a sampling frequency of 1 Hz.

Because the mapping from band-power data to stress was considered to be static, as opposed to dynamic, and because the nature of stress in response to a general stimulus is not binary, a regression tool in Matlab was used to train this approximator.

The data from stage one (band-power and ground truth stress) were each divided into two parts: a training data set, containing the first $\frac{2}{3}$ of stage one run-time, and a test data set, containing the final $\frac{1}{3}$. The training data was then used to train a

regression model using the 70 band-power data points as inputs, and the ground truth stress value as an output. Four Gaussian process models performed roughly equally, producing a root-mean-square error of ~ 0.33.

After training the regression models, they could subsequently be validated using the test data set using the recorded band-power data. While the predicted stress signal (henceforth referred to as "approximated stress") did capture the trends of the ground truth stress value, it was excessively noisy for each model and required filtering for any future use. Unfortunately, our purposes required very little (preferably zero) delay. This ruled out traditional IIR filtering methods (Chebyshev, Butterworth, etc.). In addition, due to the passband requirements, any traditional FIR filter methods that met the desired magnitude response (windowing desired impulse response, equiripple, weighted least-squares, etc.) produced a delay that was too large. Thus, a Savitzky-Golay smoothing filter was used to capture the trends and eliminate excessive noise. The approximated stress, before and after filtering, as well as the ground truth stress, can be seen in Fig. 3.5.

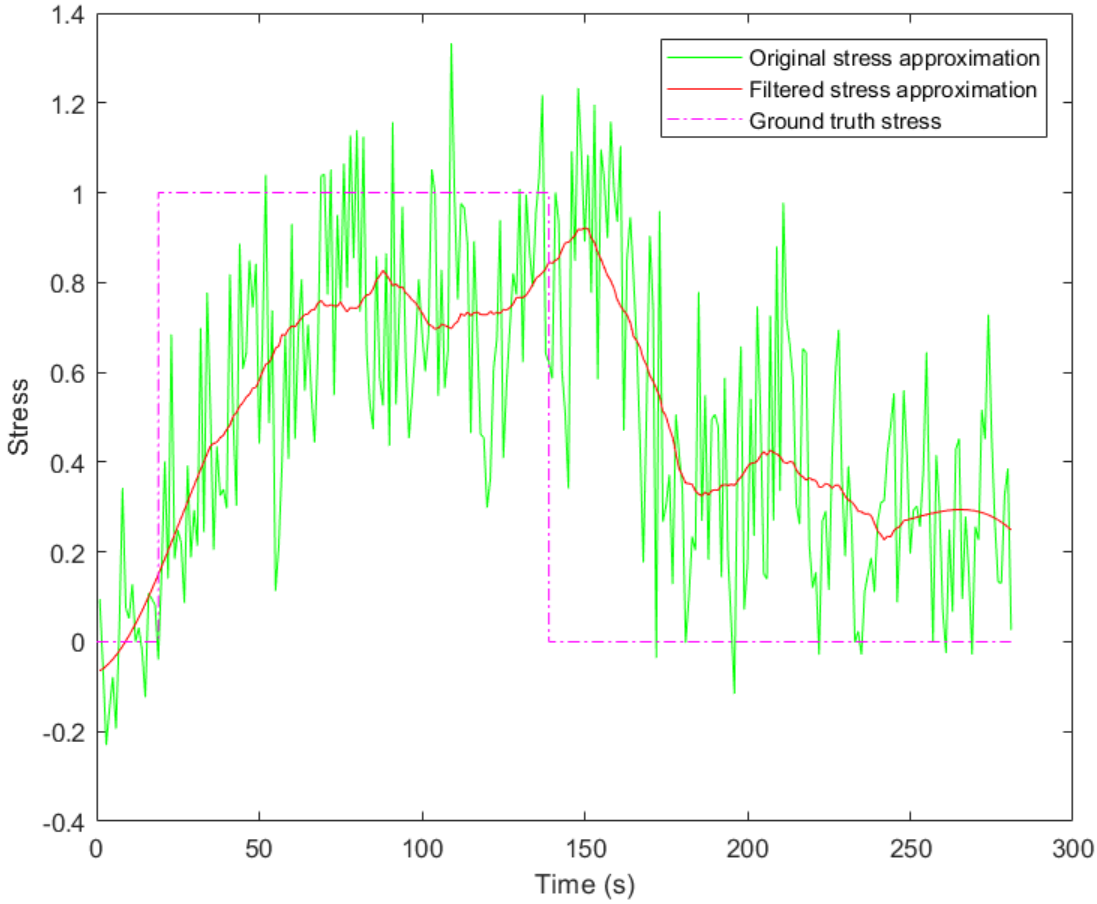

Figure 3.5: Approximated stress, before and after filtering, and ground truth stress vs. time.

Clearly, this stress approximation is able to track changes in stimuli, and could then be used in characterizing the relationship between music and stress.

Music to Stress

After calibrating the mapping between EEG band-power data and stress for a subject, the relationship between a musical stimulus and stress could be investigated.

This subsystem is shown in Fig. 3.6, and uses data captured from stage two of the experiment.

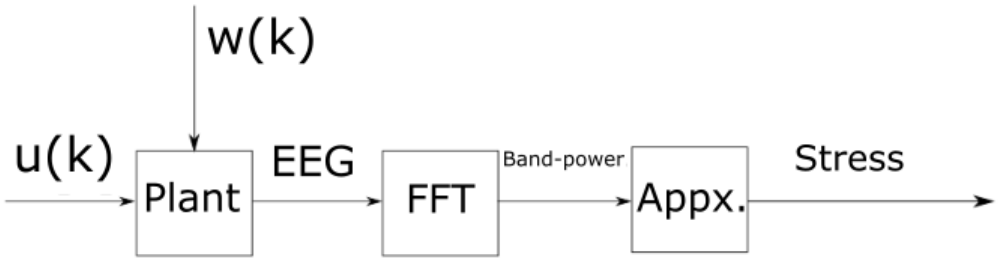

Figure 3.6: Music to stress configuration.

Before evaluating this system, the band-power data from stage two was again decimated to 1 Hz and was used to approximate a stress signal using the regression models trained in the previous section. Then, like the data from stage one, this data from stage two (approximated stress, audio pitch, audio volume) was divided into a training data set containing the first $\frac{2}{3}$ and a test data set containing the final $\frac{1}{3}$ of the stage two run time.

Because the relationship between music and stress was considered to be dynamical, as opposed to the static relationship considered before, a system identification tool was necessary to produce a model. Thus, the System Identification app in Matlab was used to estimate two fourth-order linear discrete-time single-input-single-output state-space models from the training data set: the first system mapping the relationship between the average pitch of the audio to approximated stress, and the second mapping the relationship between average volume of the audio to approximated stress.

Pitch

First, the average pitch and approximated stress signals from the training data sets were used to estimate a state-space model, which can be described by the following equations, where $y(k)$ is the approximated stress, $u_p(k)$ is the average pitch of the audio stimulus, and $x(k)$ can then be considered as an internal state of the system:

$$x(k+1) = \begin{bmatrix} x_1(k+1) \\ x_2(k+1) \\ x_3(k+1) \\ x_4(k+1) \end{bmatrix} = \Phi_p x(k) + \Gamma_p u_p(k)$$

$$= \begin{bmatrix} -0.0003 & 0.0360 & -0.2457 & -0.0244 \\ -0.0118 & -0.0490 & 2.0587 & 0.0585 \\ -0.0181 & -0.5271 & -9.6382 & -2.5112 \\ -0.0429 & -0.0371 & 1.0813 & 0.2460 \end{bmatrix} x(k) + \begin{bmatrix} 0.0032 \times 10^{-3} \\ -0.0119 \times 10^{-3} \\ 0.1261 \times 10^{-3} \\ 0.0301 \times 10^{-3} \end{bmatrix} u_p(k)$$

$$y(k) = H_p x(k) + J_p x(k)$$

$$= \begin{bmatrix} -2.7173 & 0.0075 & -0.1508 & -0.0151 \end{bmatrix} x(k) + \begin{bmatrix} 0 \end{bmatrix} u_p(k)$$

As with most systems, $J_p = 0$, indicating that the pitch of the audio stimulus has no immediate effect on the approximated stress.

By computing the eigenvalues of Φ_p we can observe whether or not the system is asymptotically stable:

$$\begin{bmatrix} -9.2326 \\ -0.3227 \\ 0.1331 \\ -0.0194 \end{bmatrix}$$

It seems that the indication of instability is only due to the lack of quality of the identification.

Because these eigenvalues do not all lie within the unit disk, the system is not asymptotically stable. Intuitively, it can possibly be interpreted that a step input of

pitch is not enough to produce a stable level of stress–a signal of varying pitch may be necessary.

The estimated model can then be validated using the test data set. A plot of the approximated stress, computed directly from the band-power data, as well as the approximated stress from this pitch model is shown in Fig. 3.7.

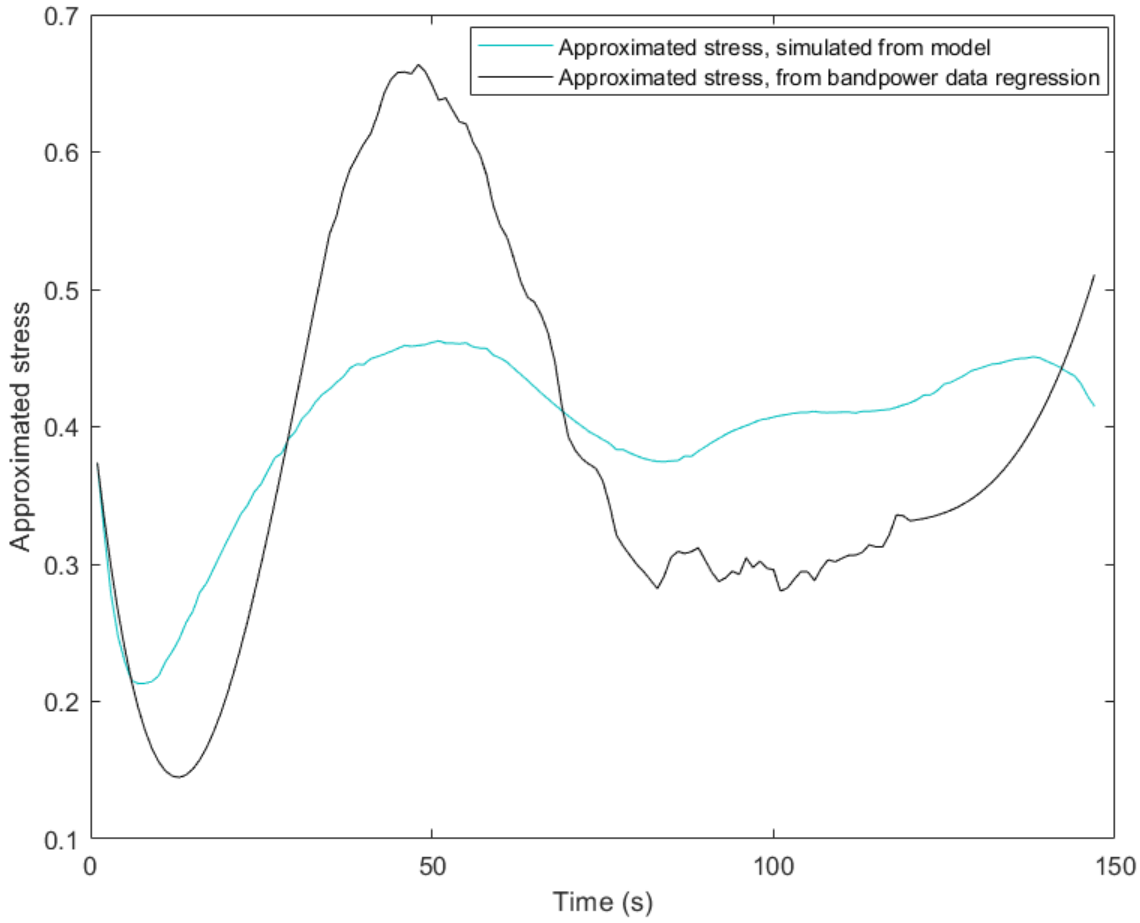

Figure 3.7: Approximated stress from band-power data and from pitch model simulation vs. time.

While the output from this system simulation does not perfectly match the approximated stress computed directly from the band-power data, it is apparent that the simulation is able to follow the general trends, with an initial minima around ~ 10 s, rising to a maximum near $\sim$ 50s, and decreasing again before increasing towards the end of the run-time.

If, instead of simulating the system completely independently of the measured stress approximation, we feed this stress approximation from the band-power data back into the system to predict future values (similar to an estimator), we observe even better tracking of the approximated stress. This can be implemented by converting the system to an auto-regressive exogeneous (ARX) model with noise e, i.e. [11]:

$$A(z)y = B(z)u + e$$

$$A(z) = 1 + \sum_{l=1}^{\infty} a(l)z^{-l},\ B(z) = \sum_{l=0}^{\infty} b(l)z^{-l}$$

Then, the m^{th}-step ahead prediction can be defined:

$$\hat{y}(k|k-m) = W_m(z)\frac{B(z)}{A(z)}u(k) + [1 - W_m(z)]y(k)$$

Where:

$$W_m(z) \triangleq \bar{H}_m(z)H^{-1}(z)$$

$$H(z) = \frac{1}{A(z)} = \sum_{l=0}^{\infty} h(l)z^{-l}$$

$$\bar{H}_m(z) = \sum_{l=0}^{m-1} h(l)z^{-l}$$

If we let $m = 5$, we can obtain the five-step prediction, as seen in Fig. 3.8.

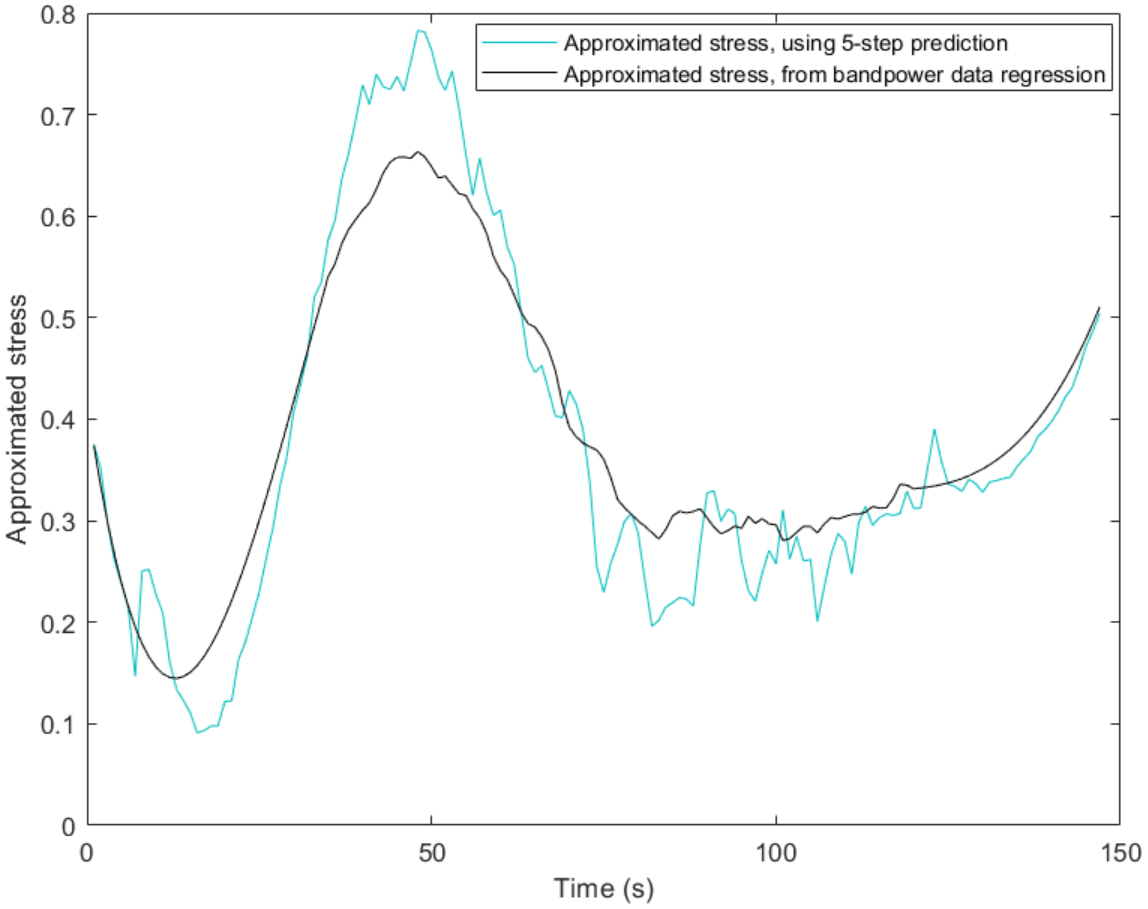

Figure 3.8: Approximated stress from band-power data and from pitch model prediction vs. time.

This five-step prediction is feasible in actual implementation, as the approximated stress can be computed if we have access to the band-power data and a trained regression model from the previous section.

Volume

As we did using average pitch as an input, we can now estimate a system model for approximated stress using average volume as the input. The model is as follows, where $u_v(k)$ is now the average volume of the audio stimulus:

$$x(k+1) = \begin{bmatrix} x_1(k+1) \\ x_2(k+1) \\ x_3(k+1) \\ x_4(k+1) \end{bmatrix} = \Phi_v x(k) + \Gamma_v u_v(k)$$

$$= \begin{bmatrix} 1.0053 & 0.0501 & -0.0066 & -0.0455 \\ -0.0169 & 0.8752 & -0.0113 & 0.5269 \\ 0.0071 & -0.1531 & 0.4118 & 0.0707 \\ 0.0027 & -0.0644 & -0.9304 & 0.1658 \end{bmatrix} x(k) + \begin{bmatrix} 0.0140 \\ -0.0122 \\ 0.1930 \\ 0.2596 \end{bmatrix} u_v(k)$$

$$y(k) = H_v x(k) + J_v x(k)$$

$$= \begin{bmatrix} -2.2969 & -0.0443 & 0.0044 & 0.0230 \end{bmatrix} x(k) + \begin{bmatrix} 0 \end{bmatrix} u_v(k)$$

Again, $J_v = 0$ as expected.

Checking the magnitudes of the eigenvalues of Φ_v, we can determine whether or not the system is asymptotically stable:

$$\begin{bmatrix} 0.9940 + j0.0240 \\ 0.9940 - j0.0240 \\ 0.2351 + j0.3935 \\ 0.2351 - j0.3935 \end{bmatrix}, \begin{bmatrix} |0.9940 + j0.0240| \\ |0.9940 - j0.0240| \\ |0.2351 + j0.3935| \\ |0.2351 - j0.3935| \end{bmatrix} = \begin{bmatrix} 0.9943 \\ 0.9943 \\ 0.4584 \\ 0.4584 \end{bmatrix}$$

Because these eigenvalues all lie within the unit disk, the system model is asymptotically stable. This implies that with any bounded input, the approximated stress will remain bounded.

The volume of the song used in this experiment ranged from 0 to about 0.16. If we consider a step response of stress vs. time for $u(k) = 0.1$, $\forall\, k > 0$ in Fig. 3.9:

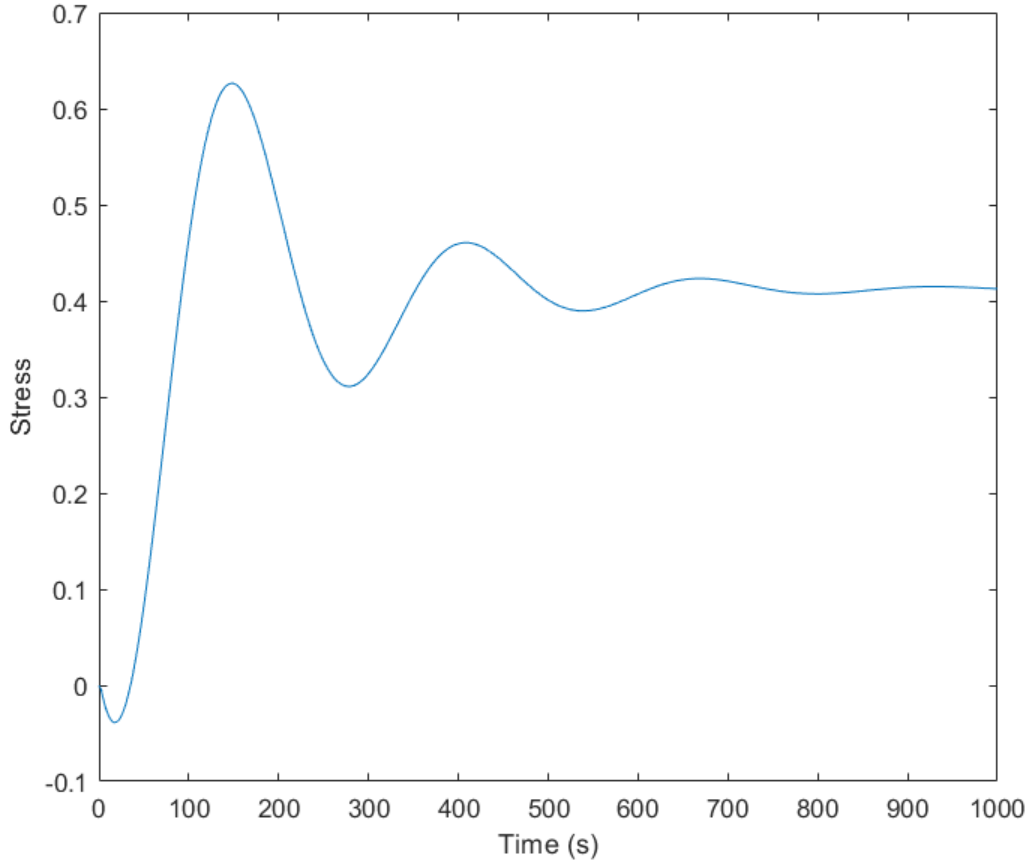

Figure 3.9: $u(k) = 0.1$ step response of volume model vs. time.

We can again validate this system model using the test data set. A plot of the approximated stress, computed directly from the band-power data, and the approximated stress from the volume model simulation, is displayed in Fig. 3.10.

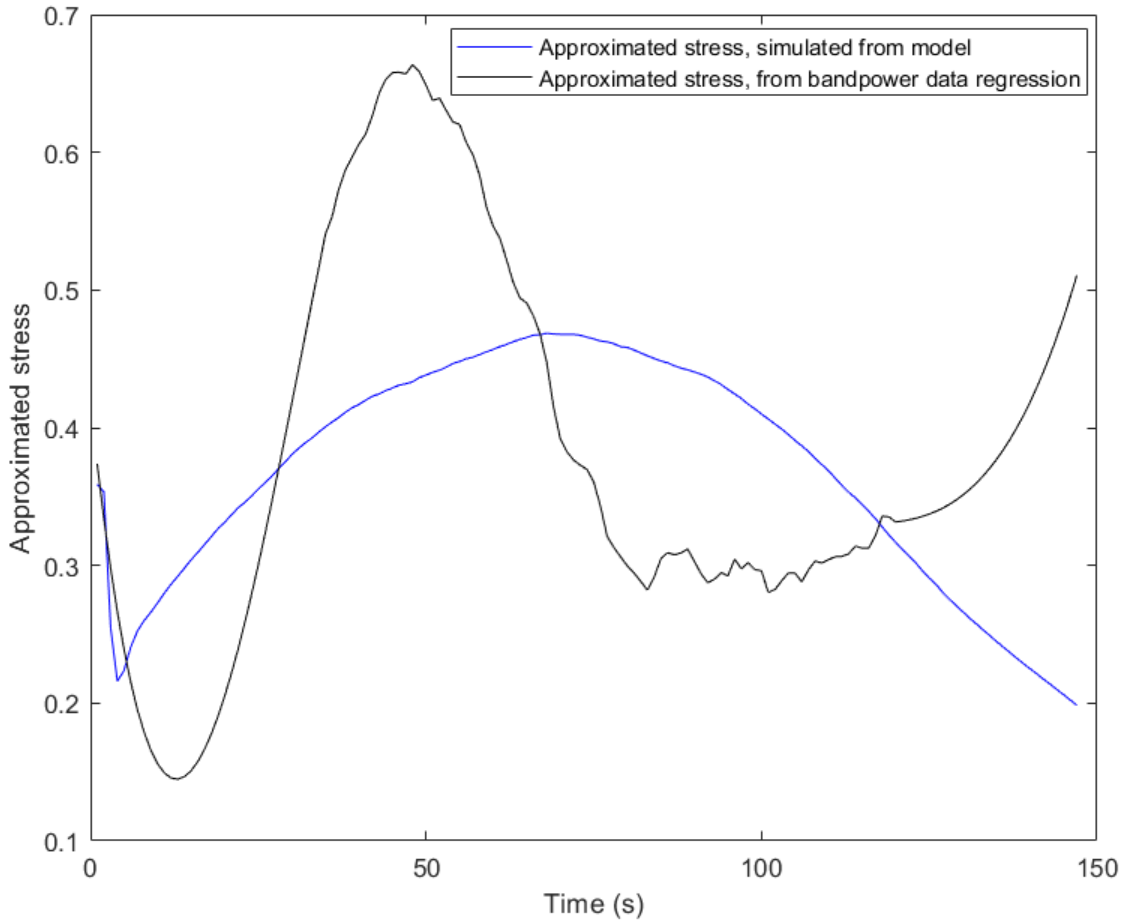

Figure 3.10: Approximated stress from band-power data and from volume model simulation vs. time.

While it is possible that this simulation output is displaying the same trends as the approximated stress from the band-power data, albeit with a substantial delay, in general the simulation output does not provide a good representation of simulated stress. Thus, it is useful to again look at the dynamics if we feed the measured approximated stress output back into the system, as did for the pitch case. The five-step prediction for this system is seen in Fig. 3.11.

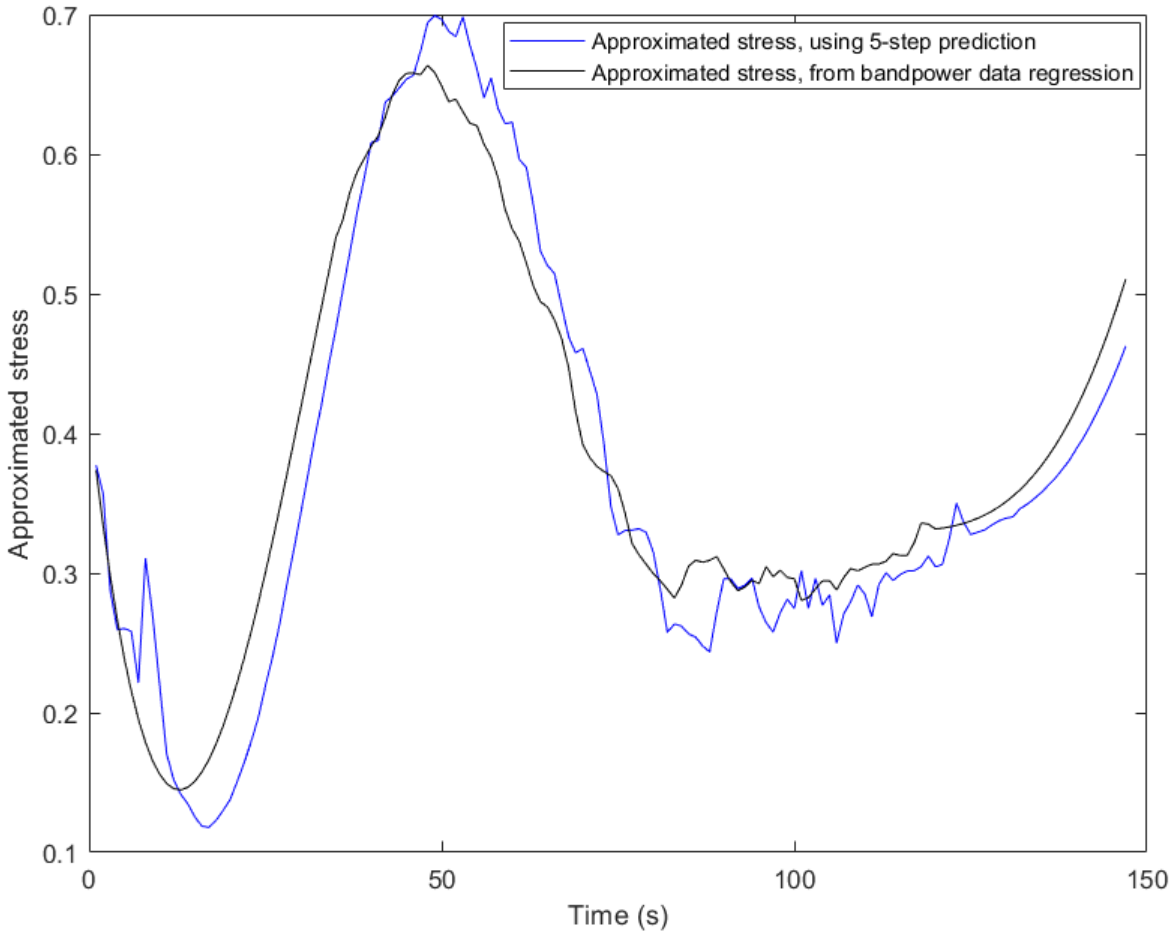

Figure 3.11: Approximated stress from band-power data and from volume model prediction vs. time.

Clearly, this predicted output from the model again does a much better job at tracking the approximated stress.

3.2 Control Implementation

Real-time Audio Modulation

If a feedback control loop is to be implemented using a for-loop in MATLAB, it is necessary to segment an audio file into fixed-length portions which can be altered by the controller and immediately streamed to a device's audio card. Fortunately, the $audioDeviceWriter()$ function in the DSP System Toolbox can load an audio signal and perform this segmentation for a user-specified length. Modulation of pitch and/or volume can then be performed, and each segment can be streamed.

Pitch

In order to shift the frequency of an audio signal up or down, the phase of each time signal must be shifted. In the discrete-time Fourier Transform (DTFT) representation of a time-domain signal, this is described by the frequency-shift property, where $a[n]$ is a time-domain audio signal, $A(e^{j\omega})$ is its DTFT counterpart, and ω_0 is a frequency shift [12]:

$$e^{j\omega_0 n}a[n] \xrightarrow{\mathscr{F}} A(e^{j(\omega-\omega_0)}$$

Fortunately, the DSP System Toolbox again provides a tool to accomplish this by applying increasing or decreasing delays to the time-domain signal, similar to the Doppler effect. The $PitchShifter$ object type allows the user to specify the pitch shift in half-steps (similar to on a piano or keyboard), and this pitch shift can be applied to the audio signal at each segment based on the feedback gain K_p that operates on the error between the reference input and stress output (proportional control). Thus, the pitch shift $u_p(k)$ can be altered at each iteration of the loop.

It is important to note that the pitch can only be shifted within a certain range before the audio becomes noticeably distorted. Thus, the gain K must be chosen such that the pitch shift never exceeds the bounds of this range.

Volume

Altering the volume of an audio signal in real time is simpler than than shifting pitch. At each time step, the volume change $u_v(k)$ can be computed as the product of the error $E(k)$ and the feedback gain K_v. Then, we can simply scale the audio signal $a[n]$, creating an increase or decrease in volume.

Preliminary Results

Proportional control tests were conducted using stress as a response to a song ("Weightless" by Marconi Union [20]). The Emotiv scaled stress value was used as the output $y(k)$ in this case, and the reference scaled stress value was chosen to be the midpoint between minimum and maximum values, $r(k) = 0.5$. A plot of the scaled stress $y(k)$ and error $E(k) = r(k) - y(k)$ can be seen in Fig. 3.12.

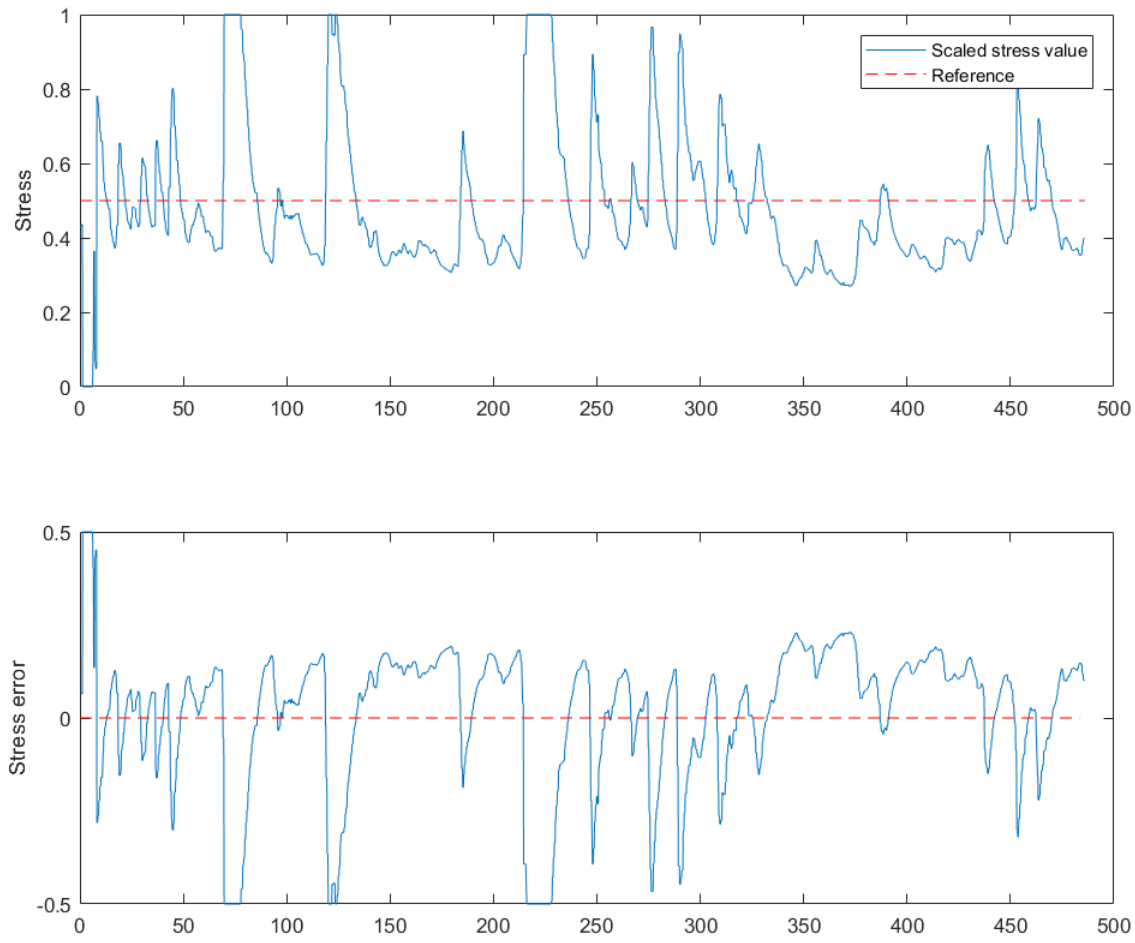

Figure 3.12: Emotiv scaled stress and error vs. time, open loop.

This open loop case shows fluctuation in stress, with a root-mean-squared error of $RMSE = 0.1874$.

When implementing a closed-loop control system with pitch modulation, the proportional gain for pitch was chosen to be $K_p = 8$. Because the error $E(k)$ has a range

from -0.5 to 0.5, the pitch shift control input $u_p(k) = K_p E(k)$ has a range of -4 to 4 half-steps. The scaled stress, error, and pitch shift are displayed in Fig. 3.13.

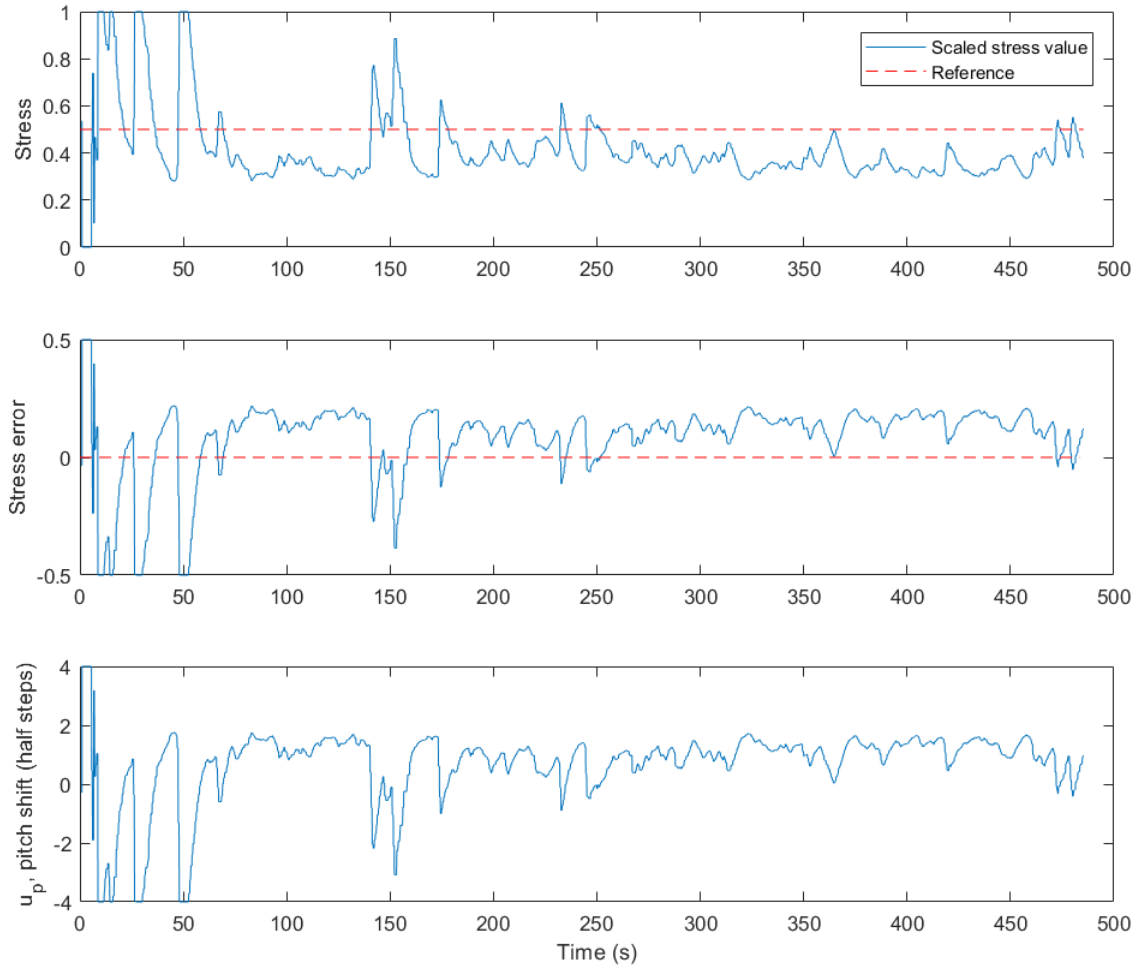

Figure 3.13: Emotiv scaled stress, error, and pitch shift u_p vs. time, $K_p = 8$.

In this closed-loop case, we see moderate improvement over the open loop case, as the scaled stress value $y(k)$ hovers just below the reference $r(k) = 0.5$ for much of the

experiment run-time. The root-mean-squared error of this controller's performance is $RMSE = 0.1758$, indicating a marginally better performance than the open-loop case.

For the case using volume modulation, the proportional gain was chosen as $K_v = 1$. Thus, the volume change had a range of -0.5 to 0.5, i.e. the amplitude of the audio signal ranged from 0.5 to 1.5 times its original amplitude. For this case, the scaled stress, error, and volume change are displayed in Fig. 3.14.

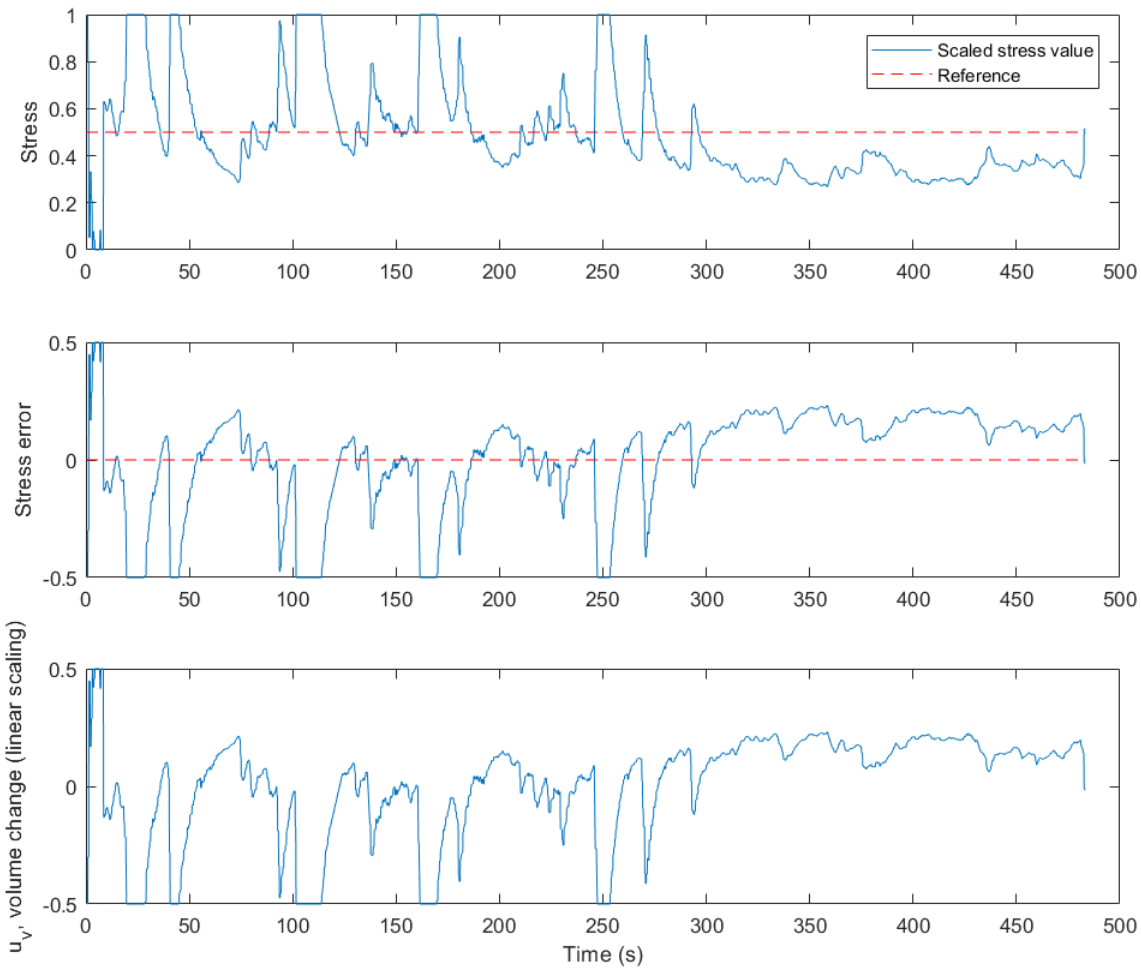

Figure 3.14: Emotiv scaled stress, error, and volume change u_v vs. time, $K_v = 1$.

This control system seems to show greater fluctuation in scaled stress than the pitch modulation system, but still generally less than the open-loop case. Despite this, the root-mean-squared error of this case is $RMSE = 0.2064$, indicating overall worse performance than even the open-loop system.

These results may indicate reasons for optimism for the use of feedback control, though it is important to recognize the ways in which the Emotiv scaled stress metric seems to fall short. In all three cases examined, the scaled stress values seem to stabilize, relatively speaking, after the first half of the experiment. This metric is "calibrated" against the minimum and maximum values in raw stress as the experiment continues, and are uniform for every user and trial. Thus, these results reinforce the utility of a prior calibration stage in experimentation, akin to the calibration of band-power to stress proposed earlier in this section, and should lead to improved performance in both closed-loop cases.

CHAPTER 4

CONCLUSION

The necessity for various approaches to evaluating the dynamics of emotion, as well as emotion regulation, have been well-established. Beginning to tackle the monumental challenges that accompany mental health issues around the globe requires a framework that is general enough to be applied to the large population of individuals who struggle with mood disorders, but versatile enough to create an impact to those to which it is applied. While EEG instruments are not inexpensive, models such as the EPOC+ are sufficiently capable for similar research purposes, while remaining low enough in price to still be relatively accessible.

Throughout the design and testing stages of this research, there were constant reminders of the non-idealities of this system. For example, it was often difficult to obtain consistent results, not only between different subjects, but also between different trials for the same subject. It is important to remember that in reality, the brain has many other inputs in addition to the audio stimuli that were presented. However, the method of calibrating a mapping between band-power data and stress can ideally be applied to any subject, given the thorough investigation and validation in literature of the Stroop Interference test. The results from the system of audio characteristics are similarly promising–the ability of the simulated pitch model in

approximating stress illustrated the clear relationship between music and stress, reinforcing claims in psychology research of the characteristics of music that affect stress. Ideally, implementing calibration and music-to-stress dynamics should improve the performance of a feedback controller over the controllers which used the Emotiv stress metric. We hope that this framework can be implemented and further validated in future research.

4.1 Future Research Directions

With a framework for feedback control in place, the logical next step is to rigorously test the effectiveness of such a feedback control system in regulating stress, using a calibrated stress approximator for each trial rather than the Emotiv stress metric. This should ideally be performed with a large pool of subjects of varying demographics.

With tools like MIRtoolbox, it is possible to compute less commonly examined characteristics of audio signals, such as timbre, key, mode, and rhythm. While these characteristics may have less intuitive relationships to stress, their investigation may yield interesting results. As such, these characteristics would have to be modulated in real-time. In addition, the framework presented in this research generally worked for a proportional feedback controller. It is recommended that this framework be extended for use with PID control or other more complex control methods.

Finally, it is important to extend the findings and methods outlined in this research to other biosensors and stimuli. In our research group alone, students are exploring

the influence of audio, light, images, virtual reality, and more, using heart rate, heart-rate variability, galvanic skin response, and EEG. Such investigations are encouraging, and essential for tackling the mental health hurdles that lie before us.

BIBLIOGRAPHY

[1] M. Bradley and P. Lang. *Handbook of Emotion Elicitation and Assessment*, chapter The International Affective Picture System (IAPS), pages 29–46. Oxford University Press, Inc., New York, 2007.

[2] E. Eich, J. Ng, D. Macaulay, A. Percy, and I. Grebneva. *Handbook of Emotion Elicitation and Assessment*, chapter Combining Music With Thought to Change Mood, pages 124–136. Oxford University Press, Inc., New York, 2007.

[3] J. Gross. *Handbook of Emotion Regulation*, chapter Emotion Regulation: Conceptual and Empirical Foundations, pages 3–20. The Guilford Press, New York, 2014.

[4] E. Inc. Emotiv epoc+ user guide. 2018.

[5] E. Inc. Emotiv insight. 2018.

[6] M. Javaid, M. Yousaf, Q. Sheikh, M. Awais, S. Saleem, and M. Khalid. Real-time eeg-based human emotion recognition. pages 182–190, 2015.

[7] J. Joorman and M. Siemer. *Handbook of Emotion Regulation*, chapter Emotion Regulation in Mood Disorders, pages 413–427. The Guilford Press, New York, 2014.

[8] P. Juslin and J. Sloboda. *The Psychology of Music*. Academic Press, Cambridge, MA, 2013.

[9] H. Kimmel and F. Hill. A comparison of two electrodermal measures of response to stress. *Journal of Comparative and Physiological Psychology*, 54:395–397, 1961.

[10] O. Lartrillot and P. Toiviainen. A matlab toolbox for musical feature extraction from audio. In *International Conference on Digital Audio Effects*, 2007.

[11] L. Ljung. *System Identification*, pages 63–72. Prentice-Hall, Inc., Upper Saddle River, NJ, 1999.

[12] A. Oppenheim and A. Wilsky. *Signals & Systems*. Prentice-Hall, Inc., Upper Saddle River, NJ, 1983.

[13] R. P. Orchestra. Borodin: String quartet no.2 in d - notturno. 1993.

[14] W. H. Organization. The world health report. 2001.

[15] PsyToolkit. Stroop effect. 2018.

[16] H. Schwilden, J. Schuttler, and H. Stoeckel. Closed-loop feedback control of methohexital anesthesia by quantitative eeg analysis in humans. *Anesthesiology*, pages 341–347, 1987.

[17] J. Taelman, S. Vandeput, A. Spaepen, and S. V. Huffel. Influence of mental stress on heart rate and heart rate variability. In *4th European Conference of the International Federation for Medical and Biological Engineering*, pages 1366–1369, Antwerp, Belgium, Dec. 2009.

[18] J. Tulen, P. Moleman, H. van Steenis, and F. Boomsma. Characterization of stress reactions to the stroop color word test. *Pharmacology Biochemistry and Behavior*, 32(2):9–15, 1989.

[19] F. S. Tyner, J. R. Knott, and W. Mayer. *Fundamentals of EEG Technology*. Lippincott Williams & Wilkins, Philadelphia, 1983.

[20] M. Union. Weightless. 2012.

[21] K. Wolitzky-Taylor, L. Bobova, R. Zinbarg, S. Mineka, and M. Craske. Longitudinal investigation of the impact of anxiety and mood disorders in adolescence on subsequent substance use disorder onset and vice versa. *Addictive Behaviors*, 37:982–985, 2012.